JOURNAL OF AGRICULTURAL AND FOOD CHEMISTRY

Article

pubs.acs.org/JAFC

Induction of Apoptosis and Cell Cycle Arrest in A549 Human Lung Adenocarcinoma Cells by Surface-Capping Selenium Nanoparticles: An Effect Enhanced by Polysaccharide–Protein Complexes from *Polyporus rhinocerus*

Hualian Wu,[†] Huili Zhu,[‡] Xiaoling Li,[†] Zumei Liu,[†] Wenjie Zheng,*[,†] Tianfeng Chen,[†] Bo Yu,[†] and Ka-Hing Wong*[,§]

[†]Department of Chemistry, Jinan University, Guangzhou 510632, China

[‡]Department of Pathology, Medical College, Jinan University, Guangzhou 510632, China

[§]Department of Applied Biology and Chemical Technology, The Hong Kong Polytechnic University, Hong Kong, China

ABSTRACT: Surface-capping agents play key roles in cellular uptake and biological activity of functional nanomaterials. In the present study, functionalized selenium nanoparticles (SeNPs) have been successfully synthesized using *Polyporus rhinocerus* water-soluble polysaccharide–protein complexes (PRW) as the capping agent during the reduction of selenium salts. The acquired monodisperse, spherical PRW-SeNPs presented desirable size distribution and stability in the solution. Moreover, PRW surface decoration significantly enhanced the cellular uptake of SeNPs via endocytosis. Exposure to PRW-SeNPs significantly inhibited the growth of A549 cells through induction of apoptosis and G2/M phase arrest (IC_{50} = 4.06 ± 0.25 μM) supported by an increase of sub-G1 and G2/M phase cell populations, DNA fragmentation, and chromatin condensation. Caspase-3/8 activation induced by PRW-SeNPs indicated that the activation of death receptors was the main cause of PRW-SeNP-induced apoptosis. Collectively, the results suggest that it is highly efficient to use PRW as a surface decorator of SeNPs to enhance cellular uptake and anticancer efficacy, and the PRW-SeNPs are potential chemopreventive agents for lung cancer therapy.

KEYWORDS: *nanodrug, selenium nanoparticles, cell cycle arrest, apoptosis*

INTRODUCTION

Chemotherapy is a main treatment method for cancer that essentially means applying cytotoxic medications to kill cancer cells or make them less active. However, chemotherapeutic agents can very often be cytotoxic to normal cells as well, resulting in side effects such as hair loss, nausea, and hematological and neurotoxic side effects. Scientists in different fields have devoted their efforts to harnessing the power of nanotechnology to improve the imaging, diagnosis, and targeted therapy of cancer treatment.[1,2] Cancer nanotechnology, a comprehensive and interdisciplinary subject, has emerged on the basic rationale that nanomaterials have novel optical, magnetic, electronic, and structural properties that are not available for individual molecules or bulk solids.[3,4] Nanotechnology offers diversified nanoscale tools for medicine. Among them, nanoparticles are rising as novel methods of drug delivery and have become a new focus of research. As delivery vehicles of anticancer drugs, nanoparticles can enhance active or passive targeting and thus increase selectivity, reduce toxicity, and prolong the half-life of drugs in the human body.[5] The size, stability, and surface properties of nanoparticles greatly affect the efficiency of their biological effects, and these characters are largely determined by the capping agents of nanoparticles.

Selenium (Se) is an essential trace element for human and animal health, and its biological functions are mainly exhibited through selenium-containing enzymes.[6] Besides its application potential for its antioxidant activity,[7] Se is also a chemopreventive and chemotherapeutic agent in various chemical forms for its special physiological properties.[8,9] In addition, the role of selenocompounds as sensitizers can make various kinds of cancer cells susceptible to some widely used chemopreventive and chemotherapeutic agents and prevent the occurrence of drug resistance in cancer cells.[10−13] The bioavailability and side effects of Se are closely related to its chemical forms; thus, it is imperative to fully characterize Se species that are highly bioavailable but produce few side-effects. Recently, Se nanoparticles (SeNPs) have drawn much attention due to their excellent bioavailability, biological activity, and low toxicity compared to organic or inorganic Se.[14−21] Studies have shown that functionalized SeNPs could be internalized by cancer cells through endocytosis and then induce cell apoptosis by triggering apoptotic signal transduction pathways.[18,22] Therefore, SeNPs are considered to be potential candidates for cancer chemoprevention and chemotherapy other than Se supplementation.

The capping agents of SeNPs can not only control the size and stability of SeNPs but also play an important role in enhancing cellular uptake, promoting cancer selectivity, and prolonging the circulation of SeNPs in physiological systems. However, the physicochemical properties of capping agents are

Received: August 11, 2013
Revised: September 20, 2013
Accepted: September 20, 2013
Published: September 20, 2013

closely related to the bioavailability of SeNPs.[23] Recently, fabrication of nanomaterials with naturally originated biomacromolecules as templates or capping agents has emerged as a hot field in biomedical nanomaterial.[15,18,20] Mushroom polysaccharide−protein complexes have been used as immunomodulating and anticancer agents in Asia for decades.[24] Apart from possessing different forms of β-D-glucan with different molecular weights, water solubilities, degrees of branching and conformation, polysaccharide−protein complexes also have imino groups originating from the proteins, triggering various biological reactions.[25,26] Due to their unique chemical structures, polysaccharide−protein complexes can be superior stabilizers of nanoparticles, protecting them to evade clearance and enhancing the stability and cell penetration. Our previous study demonstrated that surface decoration with polysaccharide−protein complexes isolated from mushroom sclerotium of *Pleurotus tuber-regium* could improve the size and stability of SeNPs and enhance their selectivity and anticancer ability toward human breast carcinoma MCF-7 cells.[18] Interestingly, the water-soluble polysaccharide−protein complexes (PRW) extracted from another mushroom sclerotium, namely, *Polyporus rhinocerus*, which is a traditional Chinese medicine for treating liver cancer, chronic hepatitis, and gastric ulcer,[27] were found to possess striking host-mediated antitumor activity on Sarcoma 180 implanted BALB/c mice and had a prominent cytotoxic effect on various human leukemic cell lines mediated by cell cycle arrest in vitro.[28] A recent study also demonstrated that PRW exhibited strong antiproliferative activity against both human breast (MCF-7) and lung (A549) carcinomas.[29]

Unlike the polysaccharide−protein complexes isolated from the sclerotium of *Pleurotus tuber-regium*, PRW has a smaller molecular weight (4×10^5 kDa) and has relatively high amounts of protein content (41.3%) and mannose content (12.1%).[28] Thus, in the present study, we are interested to determine whether the PRW can be used as a capping agent to prepare novel SeNPs. Besides, the effect of PRW surface decoration on size, stability, and anticancer efficacy, cellular uptake efficiency of SeNPs was also evaluated. In particular, the apoptosis-inducing effect and corresponding signaling pathway triggered by the PRW-SeNPs were further investigated on lung adenocarcinoma A549 cells also.

MATERIALS AND METHODS

Materials and Chemicals. Sodium selenite (Na_2SeO_3), thiazolyl blue tetrazolium bromide (MTT), 4′,6-diamidino-2-phenyindole (DAPI), Lyso Tracker Red, coumarin-6, propidium iodide (PI), and a bicinchoninic acid (BCA) kit were purchased from Sigma. A terminal transferase dUTP nick end labeling (TUNEL) assay kit was purchased from Roche Molecular Biochemicals. Substrates for caspase-3 (Ac-DEVD-AMC), caspase-8 (Ac-IETD-AFC), and caspase-9 (Ac-LEHD-AFC) were purchased from Calbiochem. Vitamin C was purchased from Guangzhou chemical reagent factory. The water-soluble polysaccharide-protein complexes (PRW) were isolated from the sclerotia of *Polyporus rhinocerus* as previously described.[28]

Preparation of PRW-SeNPs. Different volumes (0−6 mL) of aqueous PRW stock solution (0.25%) were mixed with aqueous sodium selenite solution (1 mL, 25 mM), and then Milli-Q water was added to 24 mL. Freshly prepared ascorbic acid solution (1 mL, 100 mM) was added dropwise into the mixtures under magnetic stirring, and the systems were allowed to react under room temperature in the dark for 24 h. Then the solution was dialyzed against Milli-Q water in the dark with intermittent changes of water at intervals until no Se was detected in the outer solution by ICP-AES analysis. A similar procedure was used to prepare PRW-SeNPs containing coumarin-6 except that coumarin-6 was added to the reaction system at a concentration of 4 μg/mL after the addition of 3 mL of PRW. After reacting for 24 h under room temperature in the dark, the solution was dialyzed against Milli-Q water by intermittent changes of water at intervals until no Se and coumarin-6 were detected in the outer solution. ICP-AES analysis and a fluorescent spectrophotometer were used to measure the Se and coumarin-6 in the solution, respectively.

Characterization of PRW-SeNPs. The PRW-SeNPs obtained were characterized by microscopic and spectroscopic methods including transmission electron microscopy (TEM), high-resolution TEM (HR-TEM), selected area electron diffraction (SAED), energy dispersive X-ray (EDX), dynamic light scattering (DLS), and Fourier transform infrared spectra (FT-IR). Briefly, TEM was carried out with a Hitachi (H-7650) at an acceleration voltage of 80 kV. The HR-TEM images, corresponding SAED pattern, and EDX were taken on a JEOL 2010 high-resolution TEM operated at 200 kV. A Zetasizer Nano ZS particle analyzer (Malvern Instruments Limited) was used to measure the particle size, size distribution, and stability of the nanoparticles in aqueous solution by DLS measurement. FT-IR of the samples was carried out on a FT-IR spectrometer (Equinox 55, Bruker) in the range of 4000−500 cm^{-1} using the KBr disk method.

Cell Lines and Cell Culture. The human cancer cell lines used in this study, including lung cancer cells A549, liver cancer cells HepG2, neuroblastoma cells Neuro-2a, breast adenocarcinoma cells MCF-7, and melanoma cells A375, and human normal kidney cells HK-2 were purchased from American Type Culture Collection (ATCC, Manassas, VA, USA) and maintained in DMEM supplemented with fetal bovine serum (10%), penicillin (100 U/mL), and streptomycin (50 U/mL) at 37 °C in a humidified incubator with 5% CO_2 atmosphere.

MTT Assay. The in vitro anticancer activities of PRW-SeNPs were determined by MTT assay as previously described.[30] Results were expressed as the percentage of the absorbance of treated groups relative to the control group.

In Vitro Cellular Uptake of PRW-SeNPs. To assess the difference of cellular uptake of PRW-SeNPs between cancer and normal cells, we used A549 and HK-2 cells to make quantitative analysis of the cellular uptake of coumarin-6-loaded PRW-SeNPs as previously described.[31] The cellular uptake efficiency of PRW-SeNPs was expressed as the percentage of the fluorescence of the tested wells over that of the positive control wells. The intracellular activity of coumarin-6-loaded PRW-SeNPs in A549 cells was traced with Lyso Tracker Red and DAPI staining as previously described.[32]

Flow Cytometric Analysis. The effects of PRW-SeNPs on the cell cycle distribution of A549 cells was examined by flow cytometric analysis.[33]

TUNEL-DAPI Co-staining Assay. The PRW-SeNP-induced DNA fragmentation and nuclear condensation in A549 cells was examined by TUNEL-DAPI costaining assay.[34]

Caspase Activity Assay. A549 cells were treated with PRW-SeNPs for 72 h, and then a fluorometric method was used to measure the activities of caspase-3, -8, and -9 as previously described.[33]

Statistical Analysis. All experiments were carried out at least in triplicate, and results were expressed as the mean ± SD. Statistical analysis was performed using SPSS statistical program version 13 (SPSS Inc., Chicago, IL, USA). The difference between two groups was analyzed by Student's *t* test, and the difference between three or more groups was analyzed by one-way ANOVA multiple comparisons. Difference with $P < 0.05$ (*) or $P < 0.01$ (**) was considered statistically significant.

RESULTS AND DISCUSSION

Preparation and Characterization of PRW-SeNPs. Particle size is a key factor determining nanoparticles' biological properties, such as cellular uptake, and particles ranging from 30 to 150 nm in size are more desired, especially in biological applications.[35] As a result, regulating the size of nanomaterials is of great significance. In the present study, we created SeNPs with ideal sizes by using PRW as capping agent of SeNPs in the simple redox system of selenite and ascorbic acid. Without

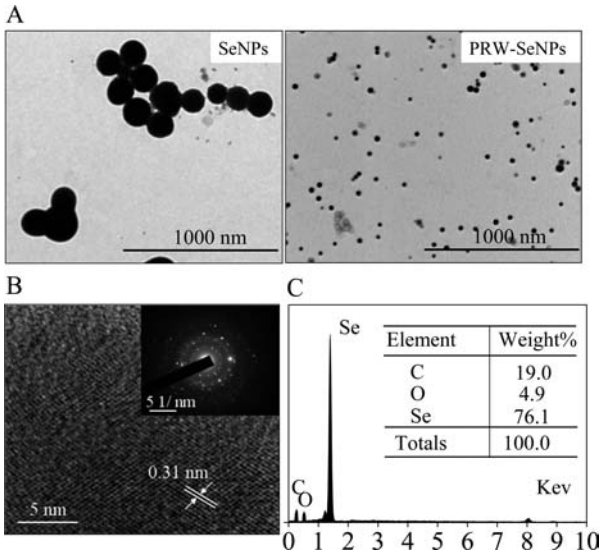

Figure 1. Representative TEM images of SeNPs without and with PRW surface decoration (A); HR-TEM images of lattice fringes (0.31 nm) and corresponding SAED pattern of PRW-SeNPs (B); representative EDX analysis of PRW-SeNPs (C). PRW-SeNPs were obtained at a concentration of 300 mg/L PRW after reacting for 24 h at room temperature in the dark.

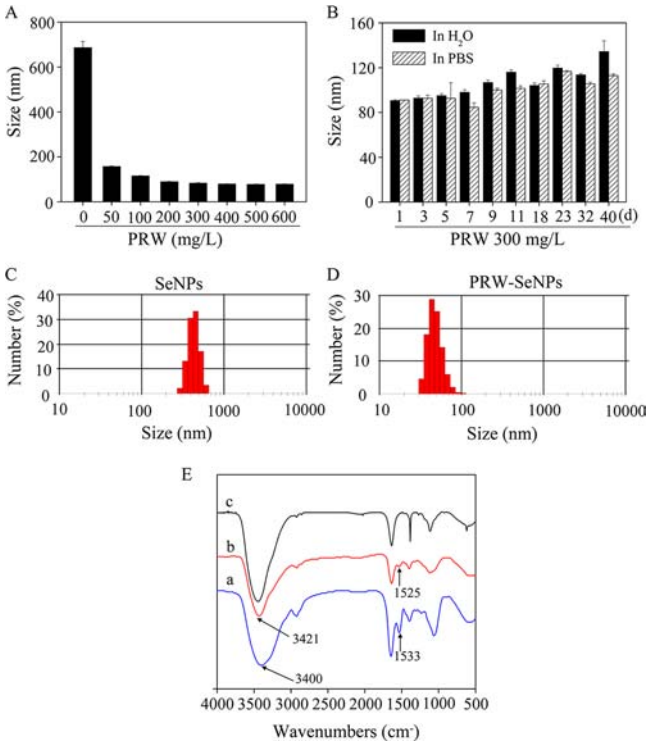

Figure 2. Relationship between particle size of SeNPs and the concentrations of PRW (A); stability of particle size of PRW-SeNPs in a time course study (B); size distribution of SeNPs (C) and PRW-SeNPs (D); FT-IR analysis of PRW-SeNPs (E): a, PRW; b, PRW-SeNPs; c, SeNPs alone. PRW-SeNPs were obtained at a concentration of 300 mg/L PRW after reacting for 24 h at room temperature in the dark.

PRW surface decoration, SeNPs can aggregate and precipitate easily (Figure 1A, left). According to the results from time course of study on particle size and polydispersity index (PDI), PRW-SeNPs presented desirable size and stability in the solution, and there were no significant differences among these concentrations (300, 400, 500, 600 mg/L) within a month (data not shown). When 300 mg/L PRW was added as capping agent, the SeNPs existed as monodispersed spherical particles in aqueous solution with an average diameter of about 50 nm (Figure 1A, right). The HR-TEM image of lattice fringes and corresponding SAED pattern of PRW-SeNPs are shown in Figure 1B. The clear lattice fringes of HRTEM image marked representatively are about 0.31 nm, indicating the nanoparticles possessed a crystal structure. The diagram from surface elemental composition analysis of PRW-SeNPs by HRTEM-EDX showed three signals, including a strong Se atom signal (76.1%) from SeNPs; minor signals of C (19.0%) and O (4.9%) probably originated from the PRW (Figure 1C).

Stability of nanomaterials is an important factor that affects their medicinal application.[36] Therefore, it is necessary to investigate the particle size, size distribution, and size stability of PRW-SeNPs. As shown in Figure 2A, the particle size of SeNPs has something to do with the concentrations of PRW. The average particle size of PRW-SeNPs was effectively controlled from 686.3 ± 28.66 (SeNPs alone) to 83.57 ± 1.79 nm at an optimal concentration of 300 mg/L PRW. Above 300 mg/L, the average particles size of PRW-SeNPs did not present significant differences, and the particle size distribution dropped from 295−615 to 33−190 nm for the control and 300 mg/L PRW groups, respectively, as shown in Figure 2C,D. The PRW-SeNPs synthesized with optimal PRW concentration (i.e., 300 mg/L) were highly water-dispersible for over 1 month, shown in Figure 2B. All of these results suggest that PRW-SeNPs possess superior characteristics and may be suitable agents for medicinal application.

The binding of PRW to SeNPs was characterized by FT-IR. The FT-IR spectra of PRW, SeNPs alone, and PRW-SeNPs are shown in Figure 2E. The absorbance peaks at 1533 and 3300−3450 cm^{-1} from the spectrum of PRW corresponded respectively to the secondary −CO−NH− group of the proteins and the stretching vibrations of hydroxyl groups of the polysaccharides. PRW-SeNPs showed a FT-IR spectrum similar to that of PRW. However, the peaks shifted from 1533 and 3400 to 1525 and 3421 cm^{-1}, respectively, indicating the interaction between the hydroxyl and imino groups from PRW complex and Se atom. These results suggest that the formation of Se−O and Se−N bonds between PRW and spherical SeNPs is the main interaction between them, leading to the highly stable spherical structure of the nanoparticles.

In Vitro Anticancer Activity of PRW-SeNPs. Active targeting of nanoparticles, a strategy of cancer nanotechnology, is usually achieved by combination of a targeting component to the surface of nanoparticles, which leads to the preferential accumulation of nanoparticles in the tumor site, individual cancer cells, or intracellular organelles inside cancer cells.[37] This technology application is based on molecular recognition, namely, specific interactions such as lectin−carbohydrate, ligand−receptor, and antibody−antigen interactions. Among them, lectin−carbohydrate and carbohydrate-based ligand−receptor are usually involved in the design of targeted drug delivery.[38,39] Research shows that the surface of cancer cells exhibits specific receptors and lectins.[37,40,41] Therefore, carbohydrate moieties usually are used in target drug delivery systems to these lectins or receptors for efficient active cancer targeting. As a kind of natural polysaccharide−protein complex, PRW is more than a targeting component, but has intrinsic

dx.doi.org/10.1021/jf403564s | J. Agric. Food Chem. 2013, 61, 9859−9866

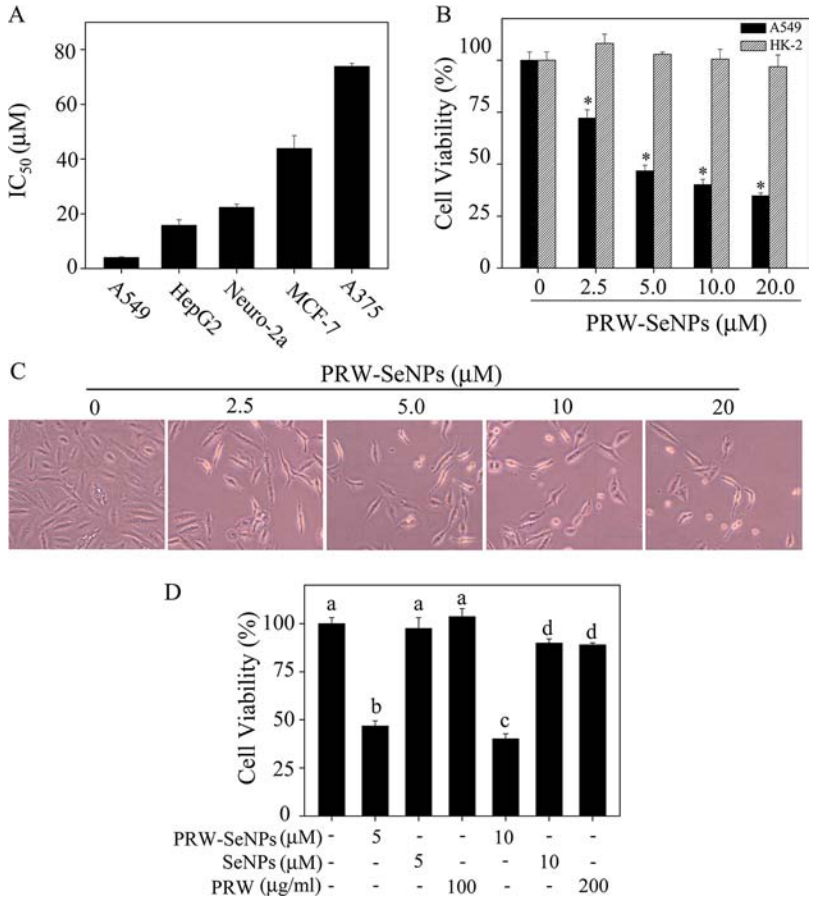

Figure 3. IC_{50} values of selected human cancer cells treated by PRW-SeNPs (A); cell viability of cancer cells A549 and normal cells HK-2 (B) and morphological changes in A549 (C); cytotoxicity of PRW-SeNPs, SeNPs, and PRW toward cancer cells A549 (D). Cells were treated for 72 h. Cell viability was determined by the MTT assay. Cells morphological changes were observed by phase-contrast microscopy (magnification, 100×).

anticancer activity. SeNPs are novel Se species possessing high anticancer activities as well. The anticancer activity of their product, PRW-SeNPs, was evaluated by MTT assay. PRW-SeNPs exhibited a broad spectrum of inhibition against several selected cancer cell lines, including A549, HepG2, Neuro-2a, MCF-7, and A375 (Figure 3A). Among them, A549 showed the highest sensitivity to PRW-SeNPs. PRW-SeNPs significantly inhibited the growth of A549 cells in a dose-dependent manner (IC_{50} = 4.06 ± 0.25 μM), but were hardly cytotoxic toward the normal kidney cells HK-2, as shown in Figure 3B. The cellular morphological changes of A549 cells exposed to PRW-SeNPs for 72 h were also examined by phase-contrast microscopy, showing dose-dependent cell number decrease, cell shrinkage, loss of intercellular contact, and formation of apoptotic bodies, whereas the control group retained its number and shape (Figure 3C). These results suggest that the cytotoxicity of PRW-SeNPs was cancer-specific.

To better illustrate the effect of PRW surface decoration on the anticancer activity of SeNPs, the cytotoxicity of PRW-SeNPs and SeNPs against A549 cells at concentrations of 5 and 10 μM was further compared. As shown in Figure 3D, PRW-SeNPs at a concentration of 10 μM significantly decreased the cancer cell viability to 40.1%, whereas SeNPs under the same condition achieved only a 10.2% decrease. The relatively high IC_{50} values of SeNPs (>100 μM) and PRW (>400 μg/mL) against A549 cells (data not shown) strongly suggest that PRW surface decoration is decisive to the strong anticancer activity of SeNPs against A549 cells.

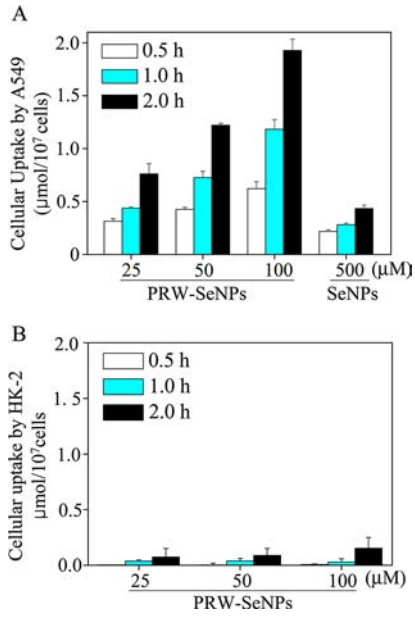

Figure 4. Quantitative analysis of cellular uptake efficiency of coumarin-6-loaded PRW-SeNPs and SeNPs by A549 cells (A) and only PRW-SeNPs by HK-2 cells (B). After 0.5, 1.0, and 2.0 h of incubation at indicated concentrations of coumarin-6-loaded nanoparticles for 37 °C, the cells were lysed in 0.2 M NaOH solution (0.5% Triton X-100). The fluorescence intensity of the solution was determined by fluorometry.

dx.doi.org/10.1021/jf403564s | J. Agric. Food Chem. 2013, 61, 9859−9866

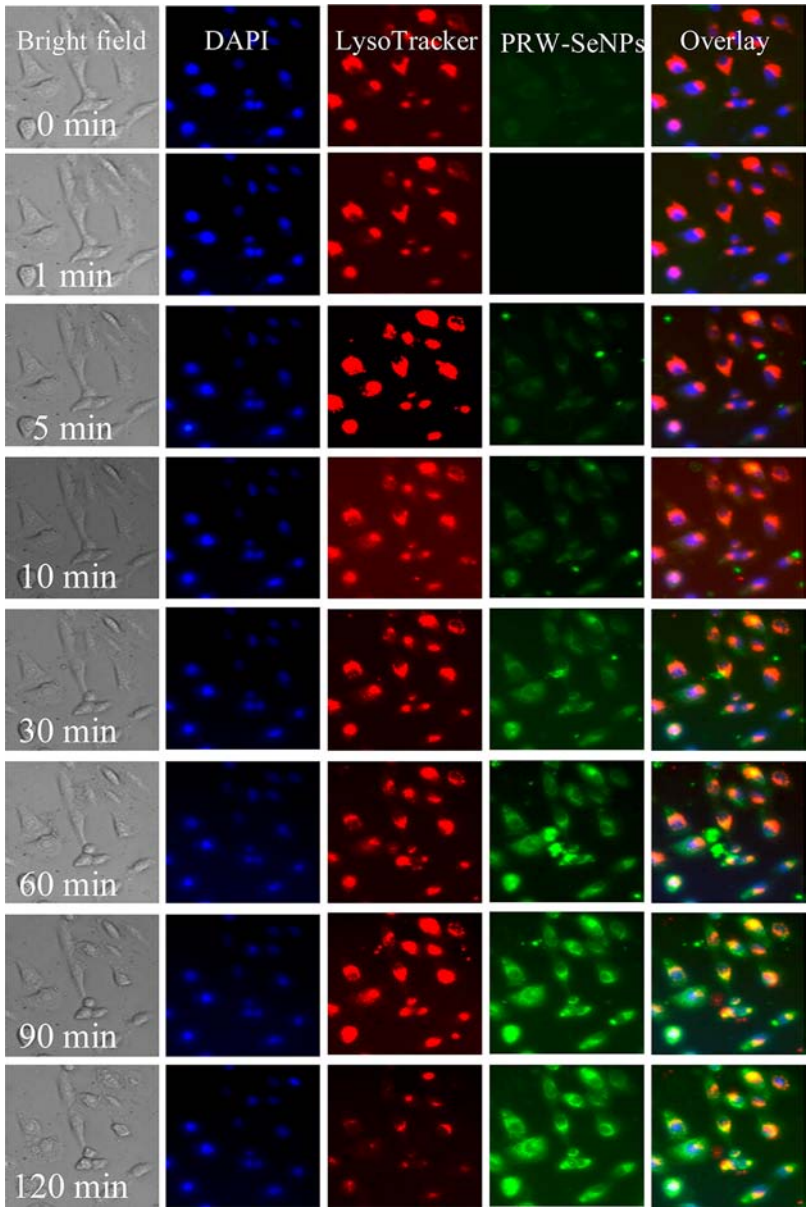

Figure 5. Cellular uptake and intracellular localization of PRW-SeNPs in A549 cells. Cells were exposed to DAPI (nucleus, blue fluorescence), Lyso Tracker Red (lysosomes, red fluorescence), and coumarin-6-loaded nanoparticles (100 μM) at 37 °C for indicated times and then visualized under a fluorescence microscope (magnification, 200×).

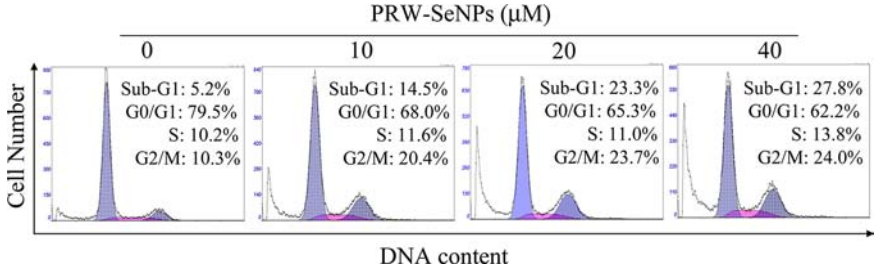

Figure 6. Flow cytometric analysis of cell cycle distribution of A549 cells. A549 cells exposed to indicated concentrations of PRW-SeNPs for 72 h were collected and stained with PI after ethanol fixation. Following flow cytometry, cellular DNA histograms were analyzed by the MultiCycle software.

In Vitro Cellular Uptake and Localization of PRW-SeNPs. To achieve a nanomaterial-based anticancer therapeutic effect, the nanoparticles absorbed into cancer cells must reach a relatively high level of concentration. Targeting nanoparticles created for cancer treatment are more likely to be absorbed into cancer cells than normal cells to reach therapeutic concentration and have greater potential to become a candidate for anticancer agents. In the present study, A549 and HK-2 cells

dx.doi.org/10.1021/jf403564s | J. Agric. Food Chem. 2013, 61, 9859−9866

were used to determine the selectivity of PRW-SeNPs between cancer and normal cells. Intracellular PRW-SeNP concentrations increased in a time- and dose-dependent manner in A549, as shown in Figure 4A. After 0.5, 1.0, and 2.0 h of treatment with 100 μM coumarin-6-loaded nanoparticles, the intracellular concentrations of PRW-SeNPs increased to 0.62 ± 0.07, 1.18 ± 0.09, and 1.93 ± 0.11 μmol/10^7 cells, respectively, which were about 2.8−4.5 times that of 500 μM SeNPs without PRW surface decoration. On the contrary, few PRW-SeNPs were absorbed into HK-2 cells (Figure 4B). These results revealed that PRW surface decoration efficiently enhances internalization of SeNPs into A549 cancer cells, but exhibits minimal internalization to normal HK-2 cells.

The A549 cell line was used for further investigation of the intracellular fate of the nanoparticles. In this study, PRW-SeNPs were loaded with coumarin-6 fluorescent dye, which emits green fluorescence. The localization of PRW-SeNPs in A549 cancer cells was detected by using specific probes, Lyso Tracker Red, and DAPI, for fluorescence imaging of lysosomes and cell nucleus, respectively. As shown in Figure 5, the overlay of the blue, green, and red fluorescences clearly indicates the colocalization of PRW-SeNPs and lysosomes in A549 cells. This suggests that the main target organelle of PRW-SeNPs is lysosomes, not cell nuclei. Moreover, the concentration of PRW-SeNPs in lysosomes increased in a time-dependent manner supported by the rapid increase in green fluorescence intensity.

Induction of Apoptosis and Cell Cycle Arrest by PRW-SeNPs. Apoptosis and cell cycle arrest are the crucial mechanisms accounting for the anticancer action of Se.[6,42] However, different forms of Se have different mechanisms for anticancer activity. Flow cytometry was used to analyze cell cycle distribution of A549 cells induced by PRW-SeNPs. The representative DNA histograms clearly showed that exposure of A549 cells to different concentrations of PRW-SeNPs resulted in G2/M phase arrest and a dose-dependent increase in apoptotic population reflected by the subdiploid peaks (Figure 6). The induction of apoptosis was further confirmed by the occurrence of DNA fragmentation and nuclear codensation detected TUNEL-DAPI costaining assay. As shown in Figure 7, DNA fragmentation,

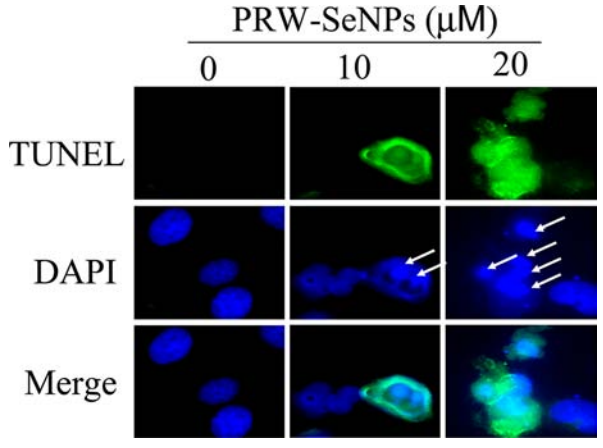

Figure 7. Representative photomicrographs of DNA fragmentation and nuclear condensation induced by PRW-SeNPs in A549 cells. After pretreatment with indicated concentrations of PRW-SeNPs for 24 h, cells were costained with TUENEL and DAPI and then observed under a fluorescence microscope (magnification, 400×).

formation of apoptotic bodies, nuclear condensation, and chromatin condensation were observed in A549 cells exposd to 10 and 20 μM PRW-SeNPs for 24. Taken together, our results suggest that apoptosis and G2/M phase arrest are the major modes of growth inhibition induced by PRW-SeNPs in A549 cells.

Induction of Caspase-Mediated Apoptosis by PRW-SeNPs. Extrinsic and intrinsic signaling pathways are the two major pathways that lead to apoptosis. In both pathways, signaling results in the activation of a family of cysteine proteases, named caspases, which are the central regulators of apoptosis. Caspase-3, -8, and -9 acted as central effectors of apoptosis and initiators of death receptor-mediated and mitochondria-mediated apoptotic pathways, respectively. To examine the possible signaling pathways involved in PRW-SeNP-induced apoptosis in A549, we measured the activities of the aforementioned initiator and effector caspases. As shown in Figure 8, exposure to 5, 10, and 20 μM

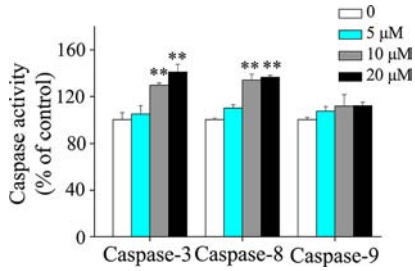

Figure 8. Caspase activation induced by PRW-SeNPs in A549 cells. Cells exposed to different concentrations of PRW-SeNPs for 72 h were collected and suspended in cell lysis buffer to obtain protein extraction. Then caspase activities were measured using synthetic fluorogenic substrates for caspase-3, caspase-8, and caspase-9.

PRW-SeNPs significantly increased the activities of caspase-3 and -8 in a dose-dependent manner. The figures from the 20 μM groups are 140.94 ± 6.71 and 136.50 ± 1.54% for caspase-3 and -8, respectively, whereas no significant change was observed for caspase-9 activities. It is thus speculated that the extrinsic pathway, namely, the death receptor-mediated pathway, was the main signaling pathway in PRW-SeNP-induced apoptosis.

In this study, a simple method for the preparation of size controllable, highly stable SeNPs decorated by PRW under a simple redox system was successfully created. SeNPs alone were easily aggregated to form bigger size and then precipitated, thus preventing their cellular uptake and biological action. In contrast, PRW surface decoration effectively reduced the diameter of SeNPs, which effectively facilitated the endocytosis and led to higher cellular uptake. Moreover, the specific interactions between PRW and biomolecules and receptors on the cancer cell membranes may play an important role in enhancing the cellular uptake of SeNPs, which increased the cytotoxicity of Se nanopartilces toward A549 cells. Studies on the underlying mechanisms revealed that the main modes of cell death induced by PRW-SeNPs were death receptor-mediated apoptosis and cell cycle arrest. Our findings in this study suggest that the use of PRW as surface decorator could be a simple approach to improve the selective uptake and anticancer action of SeNPs, and PRW-SeNPs might become potential candidates for targeted lung cancer treatment.

AUTHOR INFORMATION

Corresponding Authors

*(W.Z.) Room 643, Department of Chemistry, Jinan University, Guangzhou 510632, China. E-mail: tzhwj@jnu.edu.cn.
*(K.-H.W.) Room Y809, Department of Applied Biology and Chemical Technology, The Hong Kong Polytechnic University,

Hunghom, Kowloon, Hong Kong, China. E-mail: bckhwong@polyu.edu.hk. Phone: +86 20-85225962. Fax: +86 20 85221263.

Funding

This work was financially supported by Internal Competitive Bidding Allocation Exercise of The Hong Kong Polytechnic University, National Science and Technology Support Program of China (2012BAC07B05), Natural Science Foundation of China and Guangdong Province, Science Foundation for Distinguished Young Scholars of Guangdong Province, Program for New Century Excellent Talents in University, Research Fund for the Doctoral Program of Higher Education of China, and China Postdoctoral Science Foundation.

Notes

The authors declare no competing financial interest.

REFERENCES

(1) Heath, J. R.; Davis, M. E. Nanotechnology and cancer. *Annu. Rev. Med.* **2008**, *59*, 251−265.

(2) Surendiran, A.; Sandhiya, S.; Pradhan, S. C.; Adithan, C. Novel applications of nanotechnology in medicine. *Indian J. Med. Res.* **2009**, *130*, 689−701.

(3) Forloni, G. Responsible nanotechnology development. *J. Nanopart. Res.* **2012**, *14*, 1007−1024.

(4) Nel, A.; Xia, T.; Madler, L.; Li, N. Toxic potential of materials at the nanolevel. *Science* **2006**, *311*, 622−627.

(5) Swatantra, K. S.; Kushwaha, A. R.; Rai, A. K.; Singh, S. Novel drug delivery system for anticancer drug: a review. *Int. J. Pharm. Technol. Res.* **2012**, *4*, 542−554.

(6) Zeng, H. W. Selenium as an essential micronutrient: roles in cell cycle and apoptosis. *Molecules* **2009**, *14*, 1263−1278.

(7) Zhang, H. B.; Chen, T. F.; Jiang, J.; Wong, Y. S.; Yang, F.; Zheng, W. J. Selenium-containing allophycocyanin purified from selenium-enriched *Spirulina platensis* attenuates AAPH-induced oxidative stress in human erythrocytes through Inhibition of ROS generation. *J. Agric. Food Chem.* **2011**, *59*, 8683−8690.

(8) Chen, T. F.; Wong, Y. S. In vitro antioxidant and antiproliferative activities of selenium-containing phycocyanin from selenium-enriched *Spirulina platensis*. *J. Agric. Food Chem.* **2008**, *56*, 4352−4358.

(9) Rayman, M. P. The importance of selenium to human health. *Lancet* **2000**, *356*, 233−241.

(10) Caffrey, P. B.; Frenkel, G. D. Selenium compounds prevent the induction of drug resistance by cisplatin in human ovarian tumor xenografts in vivo. *Cancer Chemother. Pharm.* **2000**, *46*, 74−78.

(11) Li, S.; Zhou, Y. F.; Wang, R. W.; Zhang, H. T.; Dong, Y.; Ip, C. Selenium sensitizes MCF-7 breast cancer cells to doxorubicin-induced apoptosis through modulation of phospho-Akt and its downstream substrates. *Mol. Cancer Ther.* **2007**, *6*, 1031−1038.

(12) Hu, H.; Li, G. X.; Wang, L.; Watts, J.; Combs, G. F.; Lu, J. X. Methylseleninic acid enhances taxane drug efficacy against human prostate cancer and down-regulates antiapoptotic proteins Bcl-XL and survivin. *Clin. Cancer Res.* **2008**, *14*, 1150−1158.

(13) Kumi-Diaka, J.; Merchant, K.; Haces, A.; Hormann, V.; Johnson, M. Genistein-selenium combination induces growth arrest in prostate cancer cells. *J. Med. Food* **2010**, *13*, 842−850.

(14) Shen, Y. H.; Wang, X. F.; Xie, A. J.; Huang, L. C.; Zhu, J. M.; Chen, L. Synthesis of dextran/Se nanocomposites for nanomedicine application. *Mater. Chem. Phys.* **2008**, *109*, 534−540.

(15) Zhang, Y. F.; Wang, J. G.; Zhang, L. N. Creation of highly stable selenium nanoparticles capped with hyperbranched polysaccharide in water. *Langmuir* **2010**, *26*, 17617−17623.

(16) Han, J.; Guo, X.; Lei, Y. X.; Dennis, B. S.; Wu, S. X.; Wu, C. Y. Synthesis and characterization of selenium-chondroitin sulfate nanoparticles. *Carbohydr. Polym.* **2012**, *90*, 122−126.

(17) Sadeghian, S.; Kojouri, G. A.; Mohebbi, A. Nanoparticles of selenium as species with stronger physiological effects in sheep in comparison with sodium selenite. *Biol. Trace Elem. Res.* **2012**, *146*, 302−308.

(18) Wu, H. L.; Li, X. L.; Liu, W.; Chen, T. F.; Li, Y. H.; Zheng, W. J.; Man, C. W. Y.; Wong, M. K.; Wong, K. H. Surface decoration of selenium nanoparticles by mushroom polysaccharides-protein complexes to achieve enhanced cellular uptake and antiproliferative activity. *J. Mater. Chem.* **2012**, *22*, 9602−9610.

(19) Zhang, J. S.; Taylor, E. W.; Wan, X. C.; Peng, D. G. Impact of heat treatment on size, structure, and bioactivity of elemental selenium nanoparticles. *Int. J. Nanomed.* **2012**, *7*, 815−825.

(20) Yang, F.; Tang, Q. M.; Zhong, X. Y.; Bai, Y.; Chen, T. F.; Zhang, Y. B.; Li, Y. H.; Zhang, W. J. Surface decoration by *Spirulina* polysaccharide enhances the cellular uptake and anticancer efficacy of selenium nanoparticles. *Int. J. Nanomed.* **2012**, *7*, 835−844.

(21) Zheng, S. Y.; Li, X. L.; Zhang, Y. B.; Xie, Q.; Wong, Y. S.; Zheng, W. J.; Chen, T. F. PEG-nanolized ultrasmall selenium nanoparticles overcome drug resistance in hepatocellular carcinoma HepG2 cells through induction of mitochondria dysfunction. *Int. J. Nanomed.* **2012**, *7*, 3939−3949.

(22) Zhang, Y. B.; Li, X. L.; Huang, Z.; Zheng, W. J.; Fan, C. D.; Chen, T. F. Enhancement of cell permeabilization apoptosis-inducing activity of selenium nanoparticles by ATP surface decoration. *Nanomed−Nanotechnol.* **2013**, *9*, 74−84.

(23) Wu, S. S.; Su, K.; Wang, X.; Wang, D. X.; Wang, X. C.; Zhang, J. S. Protonation of epigallocatechin-3-gallate (EGCG) results in massive aggregation and reduced oral bioavailability of EGCG-dispersed selenium nanoparticles. *J. Agric. Food Chem.* **2013**, *61*, 7268−7275.

(24) Ooi, V. E.; Liu, F. Immunomodulation and anti-cancer activity of polysaccharide-protein complexes. *Curr. Med. Chem.* **2000**, *7*, 715−729.

(25) Wong, K. H.; Lai, C. K. M.; Cheung, P. C. K. Immunomodulatory activities of mushroom sclerotial polysaccharides. *Food Hydrocolloids* **2011**, *25*, 150−158.

(26) Mizuno, T.; Saito, H.; Nishitoba, T.; Kawagishi, H. Antitumor-active substances from mushrooms. *Food Rev. Int.* **1995**, *11*, 23−61.

(27) Huang, N. L. Identification of the scientific name of hurulingzhi. *Acta Edulis Fungi* **1999**, *6*, 30−32.

(28) Lai, C. K. M.; Wong, K. H.; Cheung, P. C. K. Antiproliferative effects of sclerotial polysaccharides from *Polyporus rhinocerus* Cooke (Aphyllophoromycetideae) on different kinds of leukemic cells. *Int. J. Med. Mushrooms* **2008**, *10*, 255−264.

(29) Lee, M. L.; Tan, N. H.; Fung, S. Y.; Tan, C. S.; Ng, S. T. The antiproliferative activity of sclerotia of *Lignosus rhinocerus* (tiger milk mushroom). *Evidence-Based Complement. Altern. Med.* **2012**, DOI: 10.1155/2012/697603.

(30) Chen, T. F.; Wong, Y. S. Selenocystine induces reactive oxygen species-mediated apoptosis in human cancer cells. *Biomed. Pharmacother.* **2009**, *63*, 105−113.

(31) Li, Y. H.; Li, X. L.; Wong, Y. S.; Chen, T. F.; Zhang, H. B.; Liu, C. R.; Zheng, W. J. The reversal of cisplatin-induced nephrotoxicity by selenium nanoparticles functionalized with 11-mercapto-1-undecanol by inhibition of ROS-mediated apoptosis. *Biomaterials* **2011**, *32*, 9068−9076.

(32) Yu, B.; Zhang, Y. B.; Zheng, W. J.; Fan, C. D.; Chen, T. F. Positive surface charge enhances selective cellular uptake and anticancer efficacy of selenium nanoparticles. *Inorg. Chem.* **2012**, *51*, 8956−8963.

(33) Chen, T. F.; Wong, Y. S. Selenocystine induces caspase-independent apoptosis in MCF-7 human breast carcinoma cells with involvement of p53 phosphorylation and reactive oxygen species generation. *Int. J. Biochem. Cell Biol.* **2009**, *41*, 666−676.

(34) Chen, T. F.; Liu, Y. N.; Zheng, W. J.; Liu, J.; Wong, Y. S. Ruthenium polypyridyl complexes that induce mitochondria-mediated apoptosis in cancer cells. *Inorg. Chem.* **2010**, *49*, 6366−6368.

(35) Thorek, D. L.; Tsourkas, A. Size, charge and concentration dependent uptake of iron oxide particles by non-phagocytic cells. *Biomaterials* **2008**, *29*, 3583−3590.

(36) Bakshi, M. S.; Kaur, H.; Banipal, T. S.; Singh, N.; Kaur, G. Biomineralization of gold nanoparticles by lysozyme and cytochrome C and their applications in protein film formation. *Langmuir* **2010**, *26*, 13535−13544.

(37) Sinha, R.; Kim, G. J.; Nie, S. M.; Shin, D. M. Nanotechnology in cancer therapeutics: bioconjugated nanoparticles for drug delivery. *Mol. Cancer Ther.* **2006**, *5*, 1909−1917.
(38) Gupta, A.; Gupta, R. K.; Gupta, G. S. Targeting cells for drug and gene delivery: emerging applications of mannans and mannan binding lectins. *J. Sci. Ind. Res.* **2009**, *68*, 465−483.
(39) Davis, B. G.; Robinson, M. A. Drug delivery systems based on sugar-macromolecule conjugates. *Curr. Opin. Drug Discov. Devel.* **2002**, *5*, 279−288.
(40) Lotan, R.; Raz, A. Endogenous lectins as mediators of tumor-cell adhesion. *J. Cell Biochem.* **1988**, *37*, 107−117.
(41) Monsigny, M.; Roche, A. C.; Midoux, P. Endogenous lectins and drug targeting. *Ann. N.Y. Acad. Sci.* **1988**, *551*, 399−414.
(42) Zeng, H.; Wu, M.; Botnen, J. H. Methylselenol, a selenium metabolite, induces cell cycle arrest in G1 phase and other cancer signaling genes. *J. Nutr.* **2009**, *139*, 1613−1638.